XL CILAMCE
IBERO-LATIN AMERICAN CONGRESS ON COMPUTATIONAL METHODS IN ENGINEERING
NOVEMBER 11-14, 2019
Praiamar Natal Hotel & Convention Natal, RN-BRAZIL

PARAMETERS ESTIMATION USING ABC TECHNIQUE OF MHD PULSATILE FLOW OF A NON-NEWTONIAN FLUID IN POROUS BLOOD VESSELS

Jackline Rodrigues Ferreira[2]
Fabio de Andrade Pontes[2]
Helder Kiyoshi Miyagawa[2]
Emanuel Negrão Macêdo[1]
João Nazareno Nonato Quaresma[1]
ferreira.jackline@ufpa.br
fabiopontes@ufpa.br
helderkm@ufpa.br
enegrao@ufpa.br
quaresma@ufpa.br
Diego Cardoso Estumano[3]
Nielson Fernando da Paixão Ribeiro[1]
dcestumano@ufpa.br
nielson@ufpa.br
[1]*Faculdade de Engenharia Química, Instituto de Tecnologia, Universidade Federal do Pará, FEQ/ITEC/UFPA.*
Campus Universitário do Guamá, 66075-110, Belém, PA, Brasil.
[2]*Programa de Pós-Graduação em Engenharia de Recursos Naturais da Amazônia, Instituto de Tecnologia, Universidade Federal do Pará, PRODERNA/ITEC/UFPA.*
Campus Universitário do Guamá, 66075-110, Belém, PA, Brasil.
[3]*Faculdade de Biotecnologia, Instituto de Ciências Biológicas, Universidade Federal do Pará, FBIOTEC/ICB/UFPA.*
Campus Universitário do Guamá, 66075-110, Belém, PA, Brasil.

Abstract. In this work, parameter estimates of a magnetohydrodynamic model (MDH) representing the transient pulsatile blood flow were performed, considering blood rheology as a third-degree non-Newtonian fluid, through a porous blood vessel, under the action of a magnetic field, pressure gradient and subjected to an externally imposed periodic acceleration field. The direct model (MHD) is solved by applying the Method of Lines (MOL). For the application of the inverse problem via Approximate Bayesian Computation (ABC), the sensitivity coefficient was first analyzed to define which parameters should be estimated simultaneously. The algorithm used was an adaptation of ABC SMC proposed by Toni *et. al.*, (2009), where verification was performed by simulated measurement generation at different levels of uncertainty (1%, 5%, and 10%) and considering different particle quantities (200 and 500). The results show the efficiency of this algorithm to estimate the parameters of mathematical models of this nature.

Keywords: Parameter Estimation, Approximate Bayesian Computation (ABC), Blood Flow, Non-Newtonian Fluid, Magnetohydrodynamics (MHD).

1 Introduction

Magnetohydrodynamics (MHD) is the science that studies the flow of fluids subjected to magnetic fields and evaluates the mutual interaction between the magnetic and velocity fields of electrically conductive fluids and non-magnetic, for example, ionized hot gases (plasmas) and strong electrolytes (blood) (Hide e Roberts, 1962 [1]).

Blood flow studies under the influence of an external magnetic field (commonly generated by the application of magnetic dipoles) are known as BFD (Biomagnetic Fluid Dynamics) (Higashi *et al*., 1993 [2]). Great effort has recently been put into this area, which has important potential applications in biomedical sciences, citing drug transport using magnetic particles as transport agents, reducing bleeding during surgeries, and developing magnetic cell separation devices (Andra e Nowak, 1998 [3]).

The composition of blood includes plasma (water, glucose, etc.), blood cells (red blood cells, leukocytes), platelets, among others and, although the plasma has Newtonian fluid rheology, in hematocrit (percentage of volume occupied by red blood cells in total blood volume) viscosity decreases under shear stress and therefore in relation to viscosity the blood has to be considered as a non-Newtonian fluid (Hron *et al.*, 2000 [4]). In addition, interactions of hemoglobin, cell membrane, and intercellular protein give rise to the magnetic properties of blood (Higashi *et al.*, 1993) [2]. Given this, Ellahi *et al.,* (2004) [5] stated that the hypothesis of blood as a Newtonian fluid may be valid when the blood vessels are large (arteries and veins). However, when the diameter of the blood vessel is of the same order as the red blood cells and corpuscles (arteries and capillaries), it is understood that the nature of the blood should be treated as non-Newtonian.

The human cardiovascular system causes blood to flow through the pumping action of the heart, muscle organ, which in humans and other animals produces a pulsatile pressure gradient throughout the system, so that, pressure and flow are characteristics in pulsatile profiles that vary in different parts of the arterial system (Misra *et al.,* 2008) [6]. However, some diseases are caused by excessive formation of fatty substances (cholesterol and blood clots) interfere with the way blood flows through the body, because they form a porous structure that by restricting it, can lead to more and more health problems, such as myocardial infarction (MI). Thus, there is a growing interest in the development of strategies to improve understanding of this process and, consequently, to develop ways to remediate such diseases (Ritman and Lerman, 2007) [7].

Simulation of biological systems requires knowledge of the parameters that govern these processes. However, most of these parameters have unknown values and are often impossible to measure directly, so it is necessary to estimate or infer these parameters from observed data. Given this, the inverse problem techniques based on Bayesian inference become very attractive, especially the Approximate Bayesian Computation (ABC), because they do not need to calculate the likelihood function. For example, the application of this technique to models of neurological systems (Estumano, 2016) [8], tumor growth models (Costa *et al.,* 2018) [9] and biological systems (Stumpf *et al.,* 2000) [10] can be cited, in which it was clear that the application of this Bayesian technique allowed, within a certain uncertainty, the quantification of parameters that were essential for the understanding of the studied systems.

In this context, the present work intends to use the Approximate Bayesian Computation to estimate the parameters of a pulsatile MHD transient model flow model as an incompressible fluid, third-degree non-Newtonian, through porous arteries under the action of a magnetic field and a pressure gradient. For this, simulated measurements were generated considering different levels of uncertainty and a pre-estimation analysis of the sensitivity coefficient was made to choose which parameters can be safely estimated.

2 Direct Model - MHD

The transient pulsatile laminar flow of an incompressible, non-Newtonian blood fluid through a porous blood vessel in the presence of a magnetic field and a pressure gradient is shown in Fig. 1. In this problem, blood flows in the x direction through a fully porous blood vessel with radius R and an

axial velocity u (r, t), that is, the flow is considered stable and axisymmetric, without radial and angular velocity components. It is assumed that there is no slip condition (u = 0) on the outer wall (r = R) and symmetry condition in the center of the vessel (r = 0). Blood flow is caused by the pressure gradient produced by the pumping action of the heart and affected by the body acceleration (g). It is emphasized that the effect of gravity in the radial direction is neglected.

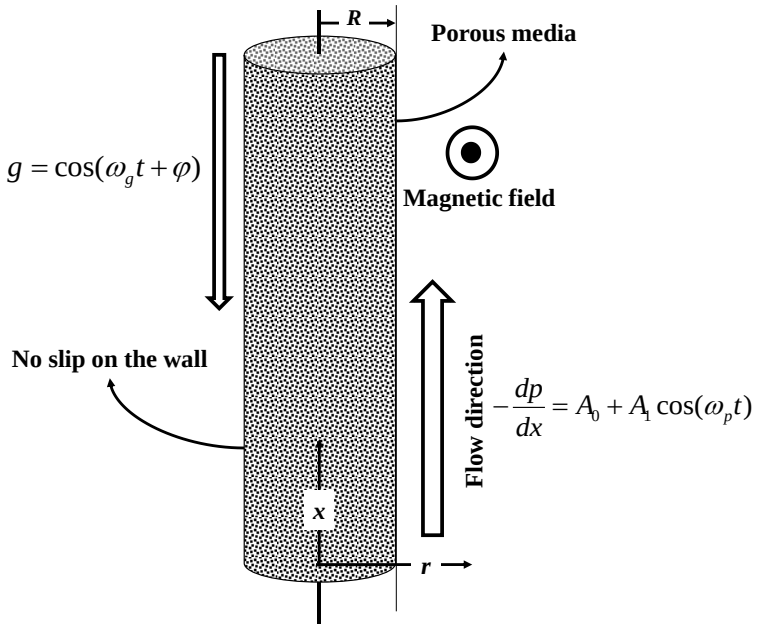

Figure 1. Conceptual physical model of MHD blood flow through a porous blood vessel (adapted from Akbarzadeh, 2016 [11]).

The dimensionless model in the domain $0 \leq r \leq 1$, $t \geq 0$ with the respective initial and boundary conditions for the velocity field was obtained by Akbarzadeh (2016) [11], as shown below:

Incorporating all simplifying assumptions into the momentum conservation equation, the governing equation direction x is expressed as Eq. (1.a):

$$\rho \frac{\partial u^*}{\partial t^*} = \{div\tau\}_x - \frac{\mu}{K} u^* - \rho A_g \cos(\omega_g t^* + \varphi) - \sigma B_o^2 u^* \tag{1.a}$$

$$\tau = -p\mathbf{I} + \left[\mu + \beta\left(tr\mathbf{A}_1^2\right)\right]\mathbf{A}_1 + \alpha_1\mathbf{A}_2 + \alpha_2\mathbf{A}_1^2 \tag{1.b}$$

$$\mathbf{A}_1 = \begin{bmatrix} 0 & 0 & \frac{\partial u^*}{\partial r} \\ 0 & 0 & 0 \\ \frac{\partial u^*}{\partial r} & 0 & 0 \end{bmatrix}; \ \mathbf{A}_2 = \begin{bmatrix} 2\left(\frac{\partial u^*}{\partial r}\right)^2 & 0 & 0 \\ 0 & 0 & 0 \\ 0 & 0 & 0 \end{bmatrix} \tag{1.c,d}$$

Where τ is the non-Newtonian stress tensor, α_1, α_2 and β are the material modules, p is the pressure, $\mathbf{A}_1$ e $\mathbf{A}_2$ are the kinematic tensors (Rivlin-Ericksen tensors), $\mathbf{I}$ is the identity matrix, K represents the permeability of the porous medium, μ is the viscosity of the blood, ρ is the specific blood mass, σB_0^2 is

the force of the magnetic field, A_o is the pressure gradient constant, A_1 is the amplitude of the pressure fluctuation that gives rise to at systolic and diastolic pressures, ω_p is the heart rate frequency ($\omega_p = 2\pi f_p$), f_p is the pulse rate, A_g is the acceleration amplitude, ω_g is the frequency ($\omega_g = 2\pi f_g$), φ is the conduction angle (or phase) and t is the time.

The dimensionless groups used in the present formulation are as follows:

$$r = \frac{r^*}{R}; u = \frac{u^*}{U_\infty}; t = \frac{\omega_p}{2\pi} t^*; \alpha^2 = \frac{\rho \omega_p R^2}{2\pi\mu}; B_1 = \frac{A_0 R^2}{\mu U_\infty}; \gamma = \frac{A_1}{A_0}; \Lambda = \frac{2\beta {U_\infty}^2}{\mu R^2};$$
$$M^2 = \frac{\sigma B_0 R^2}{\mu}; B_2 = \frac{\rho A_g R^2}{\mu U_\infty}; \omega = \frac{\omega_g}{\omega_p}; P = \frac{R^2}{K}; \frac{B_2}{B_1} = \frac{\rho A_g}{A_0} \tag{2.a,c}$$

Thus, the mathematical model of the problem in its dimensionless form accompanied by its initial and boundary conditions is written as follows:

$$\alpha^2 \frac{\partial u}{\partial t} = B_1(1+\gamma\cos 2\pi t) + \left(\frac{1}{r}\frac{\partial u}{\partial r} + \frac{\partial^2 u}{\partial r^2}\right) + \Lambda\left\{\frac{1}{r}\left(\frac{\partial u}{\partial r}\right)^3 + 3\frac{\partial^2 u}{\partial r^2}\left(\frac{\partial u}{\partial r}\right)^2\right\} + \\ -(M^2 + P) + B_2\cos(2\pi\omega t + \varphi) \tag{3.a}$$

$$u = 0 \quad \text{em } t = 0 \tag{3.b}$$

$$\frac{\partial u}{\partial r} = 0 \text{ em } r = 0 \tag{3.c}$$

$$u = 0 \quad \text{em } r = 1 \tag{3.d}$$

Where α^2 is the Womersley number, B_1 is the pressure gradient parameter, γ and Λ are the parameters of a third degree non-Newtonian fluid, M^2 is the magnetic parameter, B_2 is the acceleration parameter, ω is the frequency ratio and P is the porosity parameter.

The method of lines was used for direct model resolution, this method replaces the spatial derivatives (boundary value problem) in the partial differential equation (EDP) by algebraic approximations. Once this is done, spatial derivatives are no longer explicitly represented in terms of independent spatial variables, remaining only an initial value problem (in time). Thus, with only one independent variable remaining, a system of partial differential equations (ODEs) approximating the original EDP is obtained. Therefore, one of the main features of MOL is the use of existing and generally well-established numerical methods for ODEs (Schiesser and Griffiths, 2009) [12].

Using a regressive approximation to the derivative, the following system of ODEs is generated:

$$\alpha^2 \frac{du_i}{dt} = f(t) - (M^2 + P)u_i + \left(\frac{1}{r_i}\frac{u_i - u_{i-1}}{\Delta r} + \frac{u_{i+1} - 2u_i + u_{i-1}}{\Delta r^2}\right) + \Lambda\left\{\frac{1}{r}\left(\frac{u_i - u_{i-1}}{\Delta r}\right)^3 + \right. \\ \left. + 3\frac{u_{i+1} - 2u_i + u_{i-1}}{\Delta r^2}\left(\frac{u_i - u_{i-1}}{\Delta r}\right)^2\right\} \tag{4.a}$$

$$f(t) = B_1(1+\gamma\cos 2\pi t) + B_2\cos(2\pi\omega t + \varphi) \tag{4.b}$$

With the following initial and boundary conditions as follows:

$$\text{IC:} \quad t = 0, \qquad 0 \le r \le 1, \qquad u_i = 0 \quad 1 < i < N \tag{4.c}$$

$$\text{BC:} \quad t > 0, \qquad r = 0, \qquad u_1 = u_2 \quad i = 1 \tag{4.d}$$

$$t > 0, \qquad r = 1, \qquad u_N = 0 \quad i = N \tag{4.e}$$

3 Inverse Problem

3.1 Reduced sensitivity coefficient

The reduced sensitivity coefficient, which represents a measure of the sensitivity of the state variable Y_i in relation to the variations of the parameter P_j, was calculated by finite differences using Eq. (5). Small magnitude values of X_{ij} indicate that large variations in P_j cause small changes in u_i. In these cases, estimates of P_j parameters can be difficult since the same value of u can be obtained for a large range of P_j values. Besides the large magnitude for the sensitivity coefficient, another aspect that should be noted is linear dependence between the parameters, since it is not possible to simultaneously estimate parameters that have linearly dependent sensitivity coefficients (Beck *et al.*, 1985) [13].

$$X_{ij} = P_j \frac{\partial u_i}{\partial P_j} \approx \frac{u_i\left(P_1, P_2, ..., P_j + \varepsilon P_j, ..., P_{NP}\right) - u_i\left(P_1, P_2, ..., P_j - \varepsilon P_j, ..., P_{NP}\right)}{2\varepsilon} \tag{5}$$

3.2 Simulated Measurement Generation

Due to the difficulty in obtaining experimental data on pulsed magnetohydrodynamic flow of biofluids, as well as to evaluate the accuracy and robustness of the proposed inverse problem solution to be developed later, simulated velocity data along the length of the bed in the transient regime are used, which were obtained by solving the direct problem through specifying the parameters and imposing a disturbance with additive errors, uncorrelated Gaussians of known mean and standard deviation, as shown in Eq. (6).

$$u^{\text{measure}} = u^{\text{exact}} + \sigma^{\text{measure}} \varepsilon \tag{6}$$

In this context, it is possible to analyze three levels of uncertainty, $\sigma^{measure}$ (measure deviation): 1%, 5% and 10%, Eq. (7a-c), which represent scenarios of very well calibrated sensors or equipment (1%) even a situation where the measures have a high level of uncertainty as a function of their related errors (10%).

$$\sigma^{\text{measure}} = 0,01 \max u^{\text{exact}}; \qquad \sigma^{\text{measure}} = 0,05 \max u^{\text{exact}}; \qquad \sigma^{\text{measure}} = 0,1 \max u^{\text{exact}} \tag{7a-c}$$

3.3 Approximate Bayesian Computation (ABC)

The Approximate Bayesian Computing (ABC) technique was initially developed by Rubin (1984) [14] and Diggle and Gratton (1984) [15]. ABC is advantageous over other Bayesian techniques because it does not require the exact calculation of the likelihood function, since many problems have a mathematically and computationally intractable likelihood function (Taylor, 1954 [16]; Beaumont *et al.*, 2009 [17]; Pritchard *et al.*, 2009 [18]; Chiachio *et al.*, 2014 [19]). These ABC techniques basically follow the following algorithm:

(i) Sample a candidate parameter vector P* from some proposed a priori distribution π(**P**);

(ii) Simulate a model data set u* by solving the direct model **u*** ≡ f (**P***);

(iii) Compare the dataset, u*, with the experimental / simulated data, u, using a distance function d and a tolerance ε, if d (u, u*) ≤ ε, P * is accepted. The tolerance ε ≥ 0 is the desired level of agreement between u and u*.

Toni *et al.*, [20] presented an Approximate Bayesian Calculation algorithm based on sequential Monte Carlo (ABC-SMC) to select models and estimate parameters simultaneously, based on the acceptance-rejection test and the Euclidean distance between the prediction made by the model and the experimental measurements. In this ABC SMC algorithm, it seeks a sequential approximation of a posterior probability distribution. For this, a set of intermediate distributions are obtained, which are called populations. Each population is composed of a set of accepted particles that carry with them information of the **P** parameters to be estimated and thus give rise to a simulated dataset **u***. In this work an adaptation of the referred algorithm proposed by Toni *et al*., (2009) [20], which will be presented below, however, only the parameter estimation will be made because there is only one mathematical model, there is no need to select models.

1. Set the indicator population $pop = 0$;
2. Define the indicator particle $i = 1$;
3. Draw a parameter $\boldsymbol{P}^*$ from $\pi(\boldsymbol{P})$
   If $pop = 0$, draw $\boldsymbol{P}^{**}$ regardless of $(\boldsymbol{P})$.
   If $pop > 0$, draw $\boldsymbol{P}^*$ from the previous population $\left\{\boldsymbol{P}_{pop-1}^{(i)}\right\}$ with weight w_{pop-1} and disturb the particle to get $\boldsymbol{P}^{**} \sim K_P(\boldsymbol{P}|\boldsymbol{P}^*)$, where K_P is the disturbing kernel.
   If $\pi(\boldsymbol{P}^{**}) = 0$, returns to 3.
   Simulate a candidate data set $u^* \sim f(u|\boldsymbol{P}^{**})$;
4. Set $\boldsymbol{P}_{pop}^{(i)} = \boldsymbol{P}^{**}$ and calculate the particle weight $\boldsymbol{P}_{pop}^{(i)}$,

$$w_{pop}^{(i)} = \begin{cases} 1, & if\ pop = 0, \\ \dfrac{\pi\left(\boldsymbol{P}_{pop}^{(i)}\right)}{\sum_{J=1}^{N} w_{pop-1}^{j} K_{pop}\left(\boldsymbol{P}_{pop-1}^{(i)}, \boldsymbol{P}_{pop}^{(i)}\right)}, & if\ pop > 0 \end{cases}$$

5. If $i < N$, set $i = i + 1$, and go back to 3;
6. Normalize the accepted particle weights;
7. Set *pop* = *pop* + 1 and go back 2;
8. $CV_{pop} = \dfrac{\sigma(d_i)}{\mu(d_i)}$, *CV* is the coefficient of variation;
9. $\varepsilon = \overline{D}_{pop-1}$, ε is the tolerance;
10. If $d\ (u_0, u*) \geq \varepsilon$, and go back 3;
11. If $CV_{pop} > CV_{limit}$, and go back 2. Otherwise, stop.

4 Results and discussion

The Womersley number (α^2) is a dimensionless parameter in BFD that relates the pulsatile flow frequency (transient inertial forces) and the viscous forces and, since blood vessel diameters in the human body may differ by up to three orders of magnitude (Fung, 1997 [21]), α^2 will depend predominantly on diameter. Thus, the distinction of blood vessel type here is made in terms of the Womersley number. The parameters chosen in the present work are intended to represent a capillary vessel, which allows simulations of flow in arteries, for example. Table 1 presents the value of the reference parameters (P^{ref}) used in the simulation.

Table 1. Problem reference parameters (P^{ref}) (Akbarzadeh, 2016 [11]).

Λ	0,100
γ	0,200
ω	1,00
φ	3,100
B_1	1,440
B_2	1,400
α^2	0,005
M^2+P	0,100

4.1 Generation of simulated measures

The generation of simulated measures considering the three levels and uncertainty are presented in Fig. 2.

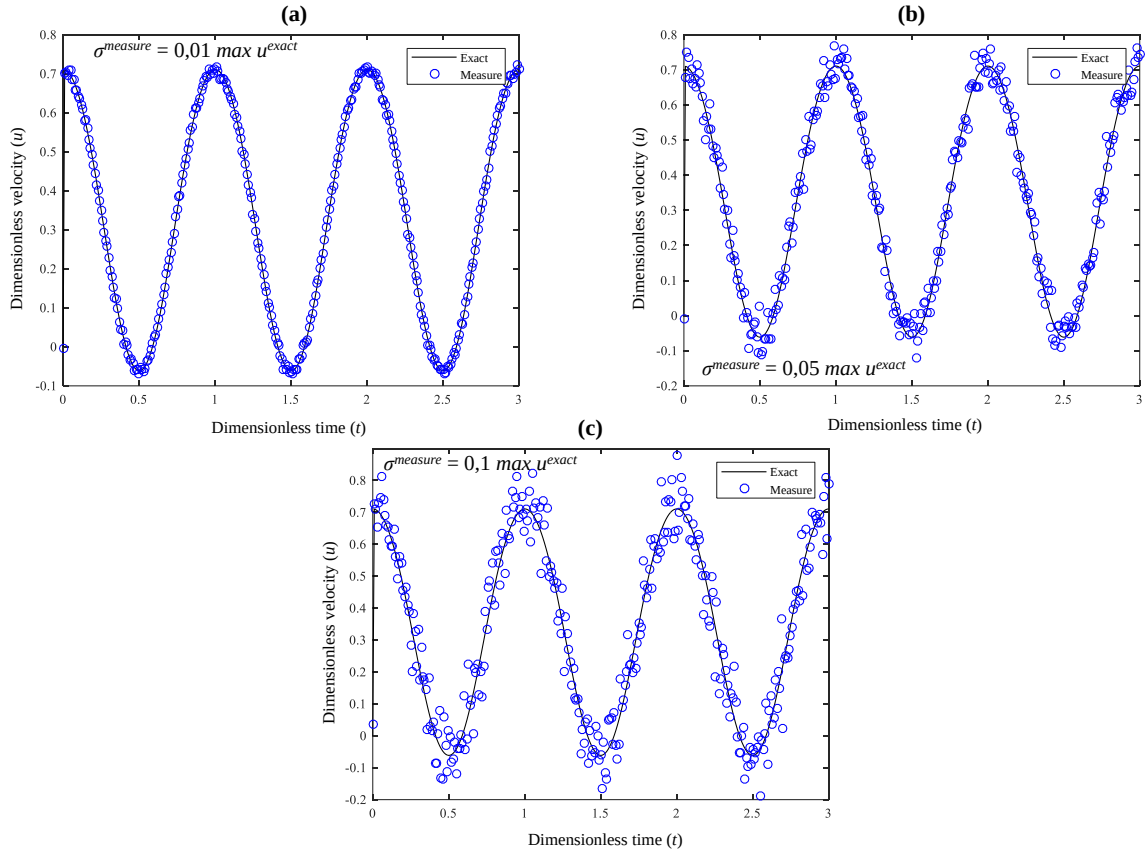

Figure 2. Velocity profile with simulated measures for MHD flow in porous capillaries for the three standard deviation values: (a) 1%, (b) 5% and (c) 10% in the central position (r = 0).

It can be observed in Fig. 2 that, for the smallest standard deviation value (1%), the simulated measure values almost coincide with the exact value obtained from the solution of the direct model, while for the other values (5% and 10%) it is already possible to notice a larger dispersion of the simulated measures in relation to the exact value, which was expected due to the nature of the normal distribution that incorporates the average in the exact value of the direct model and the value of the variance initially chosen.

4.2 Sensitivity coefficient analysis

For the sensitivity coefficient analysis, the value of the perturbation ε to be used should be evaluated, because when choosing a value too small for ε, the numerator and denominator values of Eq. (5) become very small, resulting in appearance of numerical errors. On the other hand, the use of large values ε results in approximation errors of the finite difference formula for continuous derivatives of reduced sensitivity coefficients. After evaluating the value of the perturbation, it is clear that a reasonable value that does not incorporate numerical errors or approximation errors in the results of the mathematical model analyzed here is $\varepsilon = 10^{-2}$.

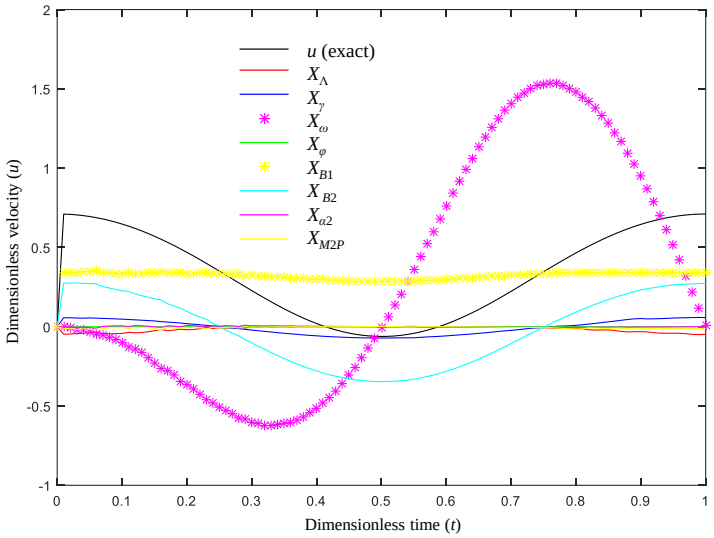

Figure 3. Analysis of reduced sensitivity coefficients of parameters Λ, γ, ω, φ, B_1, B_2, α^2 and M^2P (X_Λ, X_γ, X_ω, X_φ, X_{B1}, X_{B2}, $X_{\alpha 2}$ e X_{M2P}) with the state variable, u (r = 0).

In Fig. 3 it is possible to evaluate that the magnitude of X_Λ, X_γ, X_φ, $X_{\alpha 2}$ and X_{M2P} are very low (approximately equal to 0), so that these parameters do not have significant influence on the state variable, resulting that Λ, γ, φ, α^2 and M^2P does not need to be estimated.

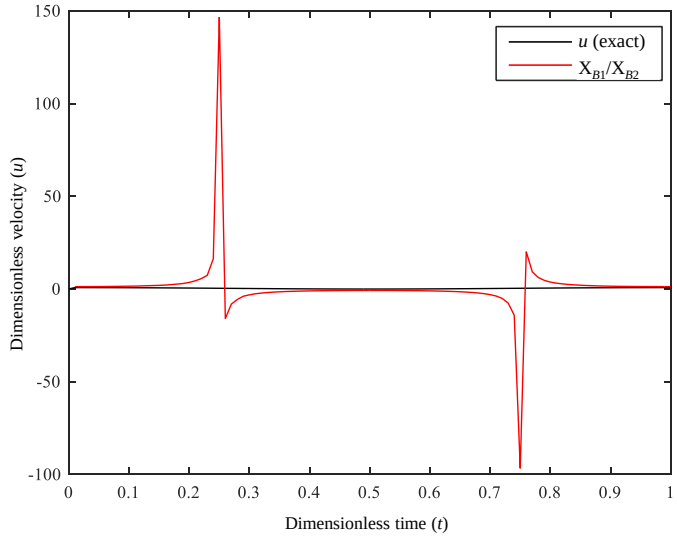

Figure 4. Ratio X_{B1}/X_{B2} plot of parameters B_1 and B_2 with state variable, u (r = 0).

In Fig. 4 it is observed that the value of the ratio X_{B1}/X_{B2} (reduced sensitivity coefficients ratio of parameters B_1 and B_2) can be considered a constant value throughout the evaluated time, since there are small intervals that present peaks down or up, indicating that both are linearly dependent. Therefore, it can be concluded that only one of the parameters, B_1 or B_2, must be estimated. Among the two, the pressure gradient parameter (B_1) is chosen to be estimated. Thus, the parameters that have the greatest

influence on the studied potential (u) and consequently the parameters to be estimated next are ω and B_1.

4.3 Parameter Estimation by ABC

Here, we analyze the variation of the measure deviation (σ_m) and the number of particles ($n_{particles}$), as shown in Table 2, so that it is possible to verify the influence of each of these on the parameter estimates. L_{inf} and L_{sup} are the limits on the uniform probability distribution: L_{inf} = 0,5*P^{ref} e L_{sup} = 1,5*P^{ref}, representing a priori probability distribution, where P^{ref} is each one of the reference parameters from Table 1. It was decided to make the parameter estimates for a period of the velocity profile (up to t = 1).

Table 2. Cases used to evaluate the influence of σ_m and $n_{particles}$ on estimates.

CASE	L_{inf} and L_{sup}	σ_m	$n_{particles}$	CV_{limit}
1	0,5 and 1,5	0,00	200	$2{,}5.10^{-1}$
2	0,5 and 1,5	0,00	500	$2{,}8.10^{-1}$
3	0,5 and 1,5	0,01	200	3.10^{-2}
4	0,5 and 1,5	0,01	500	3.10^{-2}
5	0,5 and 1,5	0,05	200	3.10^{-2}
6	0,5 and 1,5	0,05	500	3.10^{-2}
7	0,5 and 1,5	0,10	200	$2{,}5.10^{-2}$
8	0,5 and 1,5	0,10	500	3.10^{-2}
9	0,5 and 1,5	0,20	200	$2{,}5.10^{-2}$
10	0,5 and 1,5	0,20	500	3.10^{-2}

Fig. 5 presents the reduction of the parameter uncertainty with the advancement of the populations to Case 5. As all cases presented the same tendency, we chose to present only this one. Sequentially, the evolution of the state variable uncertainty is presented in Fig. 6.

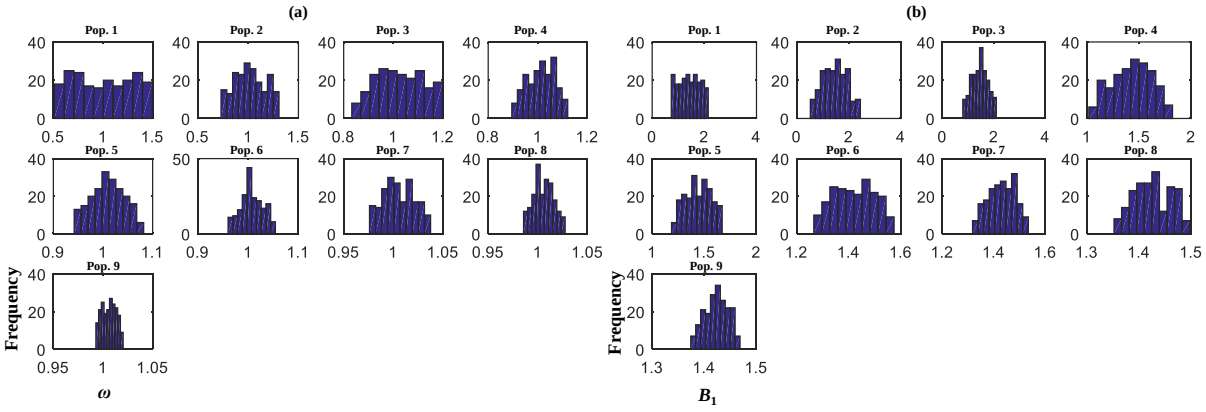

Figure 5. Population histogram evolution of the parameters (a) ω and (b) B_1 obtained from ABC estimates with $n_{particles}$ = 200 and σ_m = 5% (Case 5).

In Fig. 5, it is observed that 9 populations were necessary for the algorithm to reach the stopping criterion and that with the advancement of populations, there is a reduction in the range of the estimated parameters, which is probably a reflection of the decrease in the value of the algorithm coefficient of variation, CV, as a result of the reduction of the uncertainties associated with the parameters. The posteriori probability distribution of the parameters were, respectively, 0,95-1,05 and 1,3-1,5, considering that the exact value of the parameters, according to Table 2, were ω = 1 and B_1 = 1, 44, it can be said that the parameter estimation performed was satisfactory, since it was capable to recover the

reference parameters within a small posteriori range, from 50% to approximately ±5%, thus corroborating the assumptions of an algorithm verification.

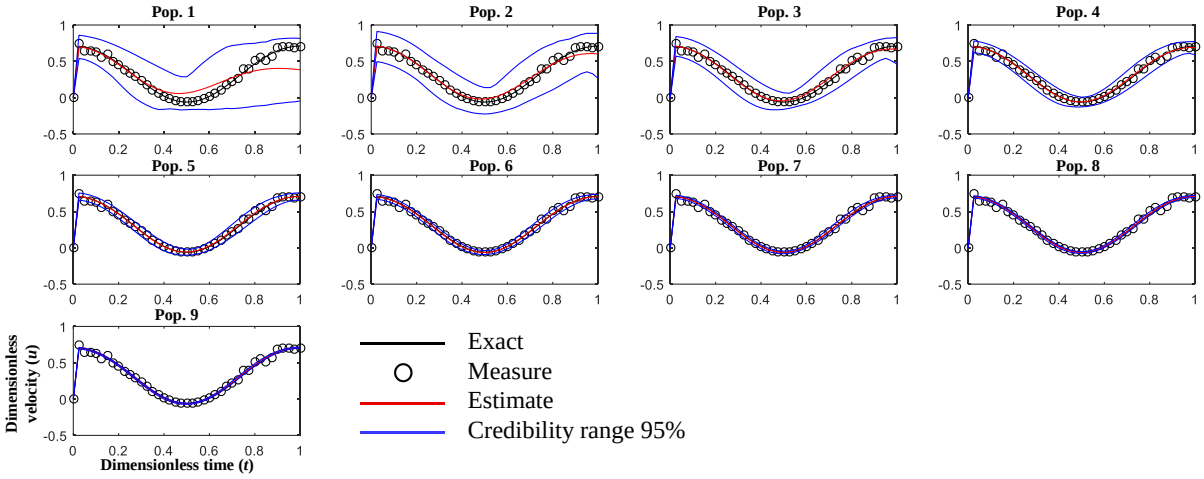

Figure 6. Evolution of velocity profiles (u) with populations to $n_{particles}$ = 200 and σ_m = 5% in the central position (r = 0) with 95% credibility range (Case 5).

Analyzing Fig. 6, we first observe the reduction of the credibility range with the advancement of populations. This occurs as a consequence of the reduction of the parameter uncertainties presented in Fig. 5, because the larger this interval is, the greater the average uncertainty of the state variable. Moreover, it can be observed that from the sixth population, the estimated state variable already presented excellent approximation compared to the simulated state variable, however, the algorithm did not stop. This was due to the requirement of the stopping criterion, the CV_{limit}, has not yet been reached. Table 3 presents the estimated parameters obtained for all cases analyzed.

Table 3. Influence of measure deviation (σ_m) and number of particles ($n_{particles}$) on estimates of ω and B_1.

CASE	σ_m	$n_{particles}$	**Number of Populations**	**Posteriori parameters interval**	
				ω **= 1**	B_1 **= 1,44**
1	0,00	200	19	0,99-1,0002	1,4395-1,4405
3	0,01	200	13	0,995-1,005	1,43-1,45
5	0,05	200	9	0,95-1,050	1,3-1,5
7	0,10	200	8	0,95-1,050	1,4-1,5
9	0,20	200	7	0,95-1,050	1-2
2	0,00	500	22	0,99-1,0000	1,4398-1,4402
4	0,01	500	13	0,995-1,005	1,43-1,45
6	0,05	500	11	0,98-1,020	1,4-1,5
8	0,10	500	7	0,95-1,050	1,2-1,6
10	0,20	500	6	0,9-1,100	1-2

Table 3 shows the influence of variation in measurement deviation (σ_m) and number of particles ($n_{particles}$) on the estimates of ω and B_1. It can be observed that, by keeping the particle number constant, increasing the measure deviation from 0 to 0,2 causes the increased uncertainty observed by the significant increase in the uncertainties of a posteriori probability distributions in the parameter histograms (last population of Fig. 5). As the measure deviation increases, there is a significant reduction in the number of populations needed to estimate both parameters (from 22 to 6 with 500 particles). This can be explained because, with greater uncertainty, the measurements become more dispersed, giving a little more freedom in comparing the calculated state variable and the measurement, so that the algorithm

needs fewer populations to meet the stopping criterion. Increasing the number of particles from 200 to 500 does not significantly change the number of populations, and the uncertainty (here measured by the posteriori interval) does not change significantly with $n_{particles}$, for the same measurement deviation in both parameters.

5 Conclusion

The algorithm used in this work was the ABC-SMC adapted from Toni *et al.* (2009) [20] to represent the flow behavior of a non-Newtonian biofluid in porous blood vessels under the action of a magnetic field, so that it can be used to simulate other cases, as well as to obtain simulated measurements.

After analyzing the reduced sensitivity coefficient, it is concluded that the frequency ratio and the pressure gradient parameter were the parameters chosen to be estimated. From the generation of simulated measures, several uncertainty scenarios were obtained and their influence on the parameters recovery was evaluated, obtaining satisfactory results for all the uncertainty levels analyzed.

The estimation of such parameters by the ABC technique demonstrates that the evaluated uncertainty scenarios produced satisfactory results, taking into account the priori probability distribution and the imposed measurement deviations. Thus, it can be concluded that this inverse problem technique was once again satisfactory for the estimation of biological parameters, a fact that is quite relevant, considering the difficulty in obtaining experimental information on these parameters. In addition, it is important to note that although this study is initial, the mathematical model used incorporated a series of hypotheses that really bring it closer to the MHD flow than the real, which compared to the vast majority available in the literature, is a differential. Thus, an important initial step for modeling and simulation of biological systems.

Acknowledgements

This work has been mainly supported by CNPQ, FAPESPA, CAPES in Procad Amazônia 2018 process number 88881.200618/2018-01.

References

[1] R. Hide and P. H. Roberts. Some Elementary Problems in Magnetohydrodynamics. *Advances in Applied Mechanics*, 1962.

[2] T. Higashi; A. Yamagishi; T. Takeuchi; N. Kawaguchi; S. Sagawa; S. Onishi and M. Date. *Blood*, v.82, p.1328, 1993.

[3] W. Andra and H. Nowak. *Magnetism in Medicine*. Wiley VCH, Berlin, 1998.

[4] J. Hron; J. Malek and S. Turek. *A numerical investigation of flows of shear-thinning fluids with applications to blood rheology*, Int. J. Numer. Methods Fluids, Vol. 32, p. 863-879, 2000.

[5] R. Ellahi; S. U. Rahman; S. Nadeem and N. S. Akbar. *Blood flow of nanofluid through an artery with composite stenosis and permeable walls*, Appl. Nanosci, vol. 4, p. 919-926, 2014.

[6] J. C. Misra; S. D. Ashikary and G.C. Shit. *Mathematical analysis of blood flow through an arterial segment with time-dependent stenosis*, Math. Model. Anal, vol. 13, p. 401-412, 2008.

[7] E.L. Ritman and A Lerman. Current Cardiology Reviews. 3, 43, 2007.

[8] D. C, Estumano. *Estimativa de parâmetros e variáveis de estado de modelos aplicados a neurônios citomegálicos utilizando dados experimentais do protocolo de tensão fixa*. Rio de Janeiro, outubro, 2016.

[9] J.M. Costa; H.R. Orlande and W. Betencurte. *Model Selection and Parameter Estimation in Tumor Growth Models Using approximate bayesian computation* – ABC, Computational and Applied Mathematics, 37(3), 2795-2815, 2018.

[10] J. Liepe; P. Kirk; S. Fillipi; T Toni; CP Barnes and M.P. Stumpf. A *framework for parameter estimation and model selection from experimental data in systems biology using approximate Bayesian computation*, Nature America 9(2), 439-456, 2014.

[11] P Akbarzadeh. *Pulsatile magneto-hydrodynamic blood flows through porous blood vessels using a third grade non-Newtonian fluids model*, Computer Methods and Programs in Biomedicine, Vol. 126, p. 3-19, 2016.
[12] W. E. Schiesser and G. W Griffiths. *A compendium of partial differential equation models: method of lines analysis with Matlab*, Cambridge University Press, New York, 2009.
[13] J.V. Beck; B. Blackwell and C.R. Clair. *Inverse Heat Conduction: ILL-Posed Problems*, Wiley Interscience, New York, 1985.
[14] D.B. Rubin. *Bayesianly justifiable and relevant frequency calculations for the applies statistician*, The Annals of Statistics 12(4),1151-1172, 1984.
[15] P.J. Diggle, R.J. Gratton. *Monte Carlo methods of inference for implicit statistical models*, Journal of the Royal Statistical Society 46(2), 193–227.7, 1984.
[16] S.G. Taylor. *The dispersion of matter in turbulent flow through a pipe*. Proceedings of The royal society 223(1155), 446-468, 1954.
[17] M.A. Beaumont; J-M Cornuet; J-M Marin and C.P. Robert. *Adaptive approximate bayesian computation*, Biometrika 96(4), 983-990, 2009.
[18] J.K. Pritchard; M.T. Seielstad; A. Perez-Lezaun and M.W. Feldman. *Population growth Y chromosomes: a study of Y choromosome microsatellities*, Mod. Biol.16(2), 1791-1798, 1999.
[19] M. Chiachio; J.L. Beck; J. Chiachio and G. Rus. *Approximate bayesian computation by subset simulation*, Siam J. Sci. Comput, 36 (3), 1339-1358, 2014.
[20] T. Toni; D. Welch and N. Strelkowa. Ipsen, M.P.H. Stumpf. *Approximate Bayesian computation scheme for parameter inerence and model selection in dynamical systems*. Journal of the royal society 6(31), 187–202, 2009.
[21] Y.C. Fung, *Biomechanics Circulation*, 2nd ed., 1997.